Evaluation de l'incertitude des courbes d'étalonnage par la méthode de Monte Carlo : Application à la turbidimétrie

Gwenaël Ruban, Claude Joannis

Evaluation of calibration curve uncertainty using the Monte Carlo method: Application to turbidity measurement

Gwenaël RUBAN*
Claude JOANNIS
LCPC-EAU, Centre de Nantes, France

ABSTRACT

Continuous measurement of the turbidity of urban wastewater is beneficial to building knowledge of pollutant flows and to the management of urban wastewater systems. Classical analytical formulas are not appropriate for evaluating the uncertainty of this type of measurement since a certain number of hypotheses are not being satisfied. In particular, the level of uncertainty on the standards might exert a significant influence. Given that a well-adapted analytical method becomes rather complex to implement within an operational framework, turbidity measurement uncertainty has been assessed herein by running calibration simulations using the Monte Carlo method. This simple and quite general method is based on the same experimental data and hypotheses as the more complex analytical method and enables explaining the causes of deviations observed with respect to the classical analytical method. Lastly, total short-term uncertainty for turbidity measurement of samples proves highly satisfactory (less than 1.5% above the 100 FAU number), provided the device has been linearized.

Évaluation de l'incertitude des courbes d'étalonnage par la méthode de Monte Carlo Application à la turbidimétrie

RÉSUMÉ

Le mesurage en continu de la turbidité des eaux résiduaires urbaines est intéressant pour la connaissance des flux de polluants et la gestion des systèmes d'assainissement urbains. Les formules analytiques classiques ne conviennent pas pour l'évaluation de l'incertitude de ce mesurage car certaines hypothèses ne sont pas satisfaites. En particulier l'incertitude sur les étalons peut jouer un rôle non négligeable. Une méthode analytique adaptée devenant alors complexe à mettre en œuvre dans un cadre opérationnel, l'incertitude de mesurage de la turbidité a été évaluée en effectuant des simulations d'étalonnages par la méthode de Monte Carlo. Cette méthode simple et générale est fondée sur les mêmes données expérimentales et les mêmes hypothèses que la méthode analytique complexe. Elle permet en outre d'expliciter les causes des écarts constatés avec la méthode analytique classique. Finalement l'incertitude totale à court terme du mesurage de la turbidité sur échantillon est très satisfaisante (moins de 1,5 % au-dessus de 100 FAU), pourvu que l'appareil soit linéarisé.

* CORRESPONDING AUTHOR:
Gwenaël RUBAN
Gwenael.Ruban@lcpc.fr

INTRODUCTION

Turbidity measurement, which is already used for measuring biomass concentrations in wastewater treatment plants, is starting to develop within drainage networks as well. This technique offers a relatively straightforward means for tracking the dynamics of particulate pollution, especially during rainfall events **[1-4]**. It may also be employed for controlling storage or treatment facilities, monitoring discharges and calibrating pollutant flow models.

For these various applications, it is preferable to know the uncertainty of turbidity measurements, particularly the uncertainty associated with the device calibration curve. In the simplest case (accurate standards, constant dispersion of recorded measurements vs. measured values), uncertainty can be calculated using either simple analytical formulas (linear device) or more complicated formulas for nonlinear devices, which often is the case for turbidity meters operating in the field **[3]**. For these devices however, the uncertainties due to measurement standards could represent a sizable proportion of total measurement uncertainty. Since analytical methods are difficult to implement within an operational framework by unspecialized personnel, the uncertainty of turbidity measurements has thus been evaluated by running calibration simulations via the Monte Carlo method.

This simple method actually proves to be well adapted when the process output variable cannot be explained by a single function of input variables, or when the uncertainty determination becomes more complex, requiring composite function differentials or in our case iterative matrix calculations.

CALIBRATION UNCERTAINTY EVALUATION USING CLASSICAL ANALYTICAL FORMULAS

Equipment, calibration and uncertainty calculation methods

› Equipment and calibration methods

A field turbidity meter has been calibrated over the range of 0-2,000 FAU (*Formazin Attenuation Units*). This range is suitable for the majority of turbidity values observed in urban wastewater. The formazine standards were prepared at the Laboratory in accordance with Standard ISO 7027 **[5]**, specific to turbidity determination. Five calibration levels of 100, 250, 500, 1,000, 2,000 FAU (in addition to the zero point), corresponding with the minimum number indicated in the standard, were obtained by means of successive dilutions of the original parent suspensions at 2,000 FAU. They were distributed into a progression with an approximately exponential trend in order to optimize relative accuracy over the lower values.

Calibration steps were performed both on a single range of standards and on five different ranges, so as to incorporate their uncertainty, as stipulated in Standard XP T 90-210 **[6]**. This standard actually pertains to the evaluation of an alternative method with respect to a reference method, yet can be transposed to sensor calibration as well. Measurements were repeated five times, once again in accordance with these standard prescriptions.

In order to increase the statistical representativeness of results, three calibration series over a single range and three series over five ranges were carried out.

› Uncertainty calculation with classical analytical formulas

The calibration uncertainty for a given standard value x_0 may be expressed by the square of the standard deviation s_{etal} (variance) according to the following expressions **[7]** (y_0 is the device indication corresponding to x_0). These expressions are valid under the hypotheses of *constant dispersion of measurement results vs. measured value* and *negligible uncertainty on the standards*.

$$s^2_{étal}(x_0) = \frac{s^2_{étal}(y_0)}{b^2} = \frac{s_I^2}{b^2}\left[\frac{1}{N} + \frac{(x_0 - xm)^2}{\sum_i n_i (x_i - xm)^2}\right] \quad (1)$$

for a calibration line with slope b and:

$$s^2_{étal}(x_0) = \frac{s^2_{étal}(y_0)}{f'(x_0)^2} = \frac{s_I^2}{f'(x_0)^2}\left[\frac{1}{N} + A_{FS}\right] \quad (2)$$

for a second-order polynomial of slope f', and with:

$$A_{F5} = \frac{A_{F1}(x_0 - xm)^2 + A_{F2}\left(x_0^2 - \frac{\sum_i n_i x_i^2}{N}\right)^2 - 2A_{F3}(x_0 - xm)\left(x_0^2 - \frac{\sum_i n_i x_i^2}{N}\right)}{A_{F4}}$$

$$A_{F1} = \sum_i n_i \left(x_i^2 - \frac{1}{N}\sum_i n_i x_i^2\right)^2 \qquad A_{F2} = \sum_i n_i (x_i - xm)^2$$

$$A_{F3} = \sum_i n_i (x_i - xm)\left(x_i^2 - \frac{1}{N}\sum_i n_i x_i^2\right) \qquad A_{F4} = A_{F1}A_{F2} - A_{F3}^2$$

where:

– s_I^2 the estimation of the residual variance (standard deviation of the square of residuals) equals $\sum_i \sum_j \left(y_{ij} - y'_i\right)^2 / (N - K)$; K is 2 for a straight line and 3 for a second-order polynomial;
– N and n_i are respectively the number of calibration values and number of repetitions for level i;
– y_{ij} and y'_i are respectively the device indications for calibration values and the corresponding ordinate of the calibration curve;
– x_i and xm are respectively the values and average of the standard values used for building the calibration curve.

The respective division by b and f'(x_0) may be simply explained by the fact that it is actually the inverse function of the calibration relation, used to convert the y_0 device indications into x_0 values expressed in terms of standard units (**Figure 1**).

Figure 1 shows an example of an adjustment on both straight line and calibration curve for the experimental points (five repetitions), with the associated uncertainty standard deviations s_{etal} (y_0) and s_{etal} (x_0) for the curve (second-order polynomial).

Figure 1
Fictitious example of calibration line and curve with the associated uncertainties (for the curve)

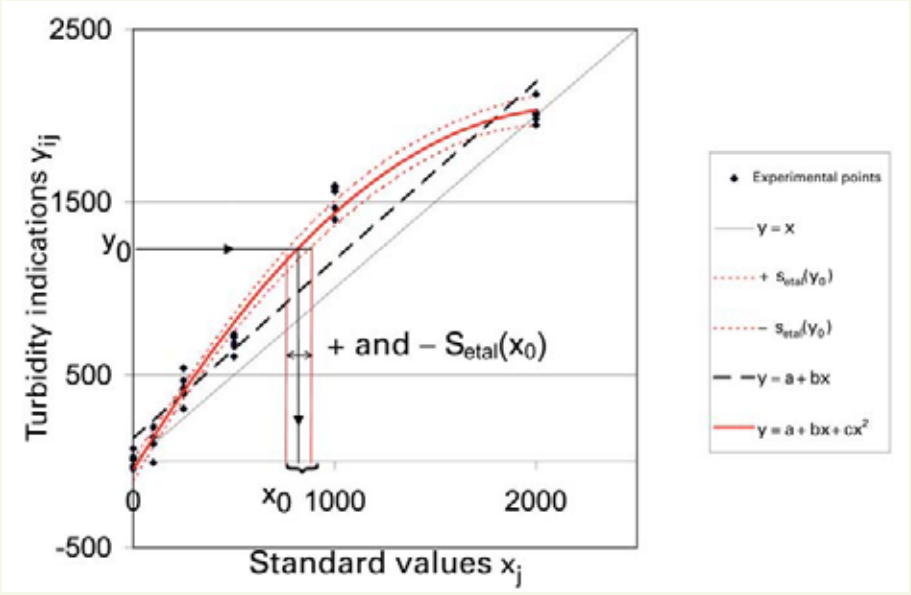

For polynomials of higher than the second order, the expression of $s^2_{etal}(x_0)$ becomes even more complex **[8]**. Various methods are proposed for determining the benefit of linearizing the device by means of a second- or higher-order polynomial. The one indicated in Standard XP T 90-210 **[6]** consists of testing whether or not the proportion of variance due to model error $\sum_i (ym_i - y'_i)^2$ exceeds the experimental error variance $\sum_i \sum_j (y_{ij} - ym_i)^2$ via the Fisher test: **Figure 2** reveals that deviations $ym_i - y'd_i$ for the straight line are greater than experimental deviations $y_{ij} - ym_i$, whereas for the second-order polynomial, the deviations $ym_i - y'p_i$ are of the same order of magnitude, which signifies that the level of experimental resolution does not enable extending to the next higher order.

Figure 2
Comparison of model errors (deviations $ym_i - y'd_i$ for the line and $ym_i - y'p_i$ for the polynomial) with the experimental error (deviations $y_{ij} - ym_i$)

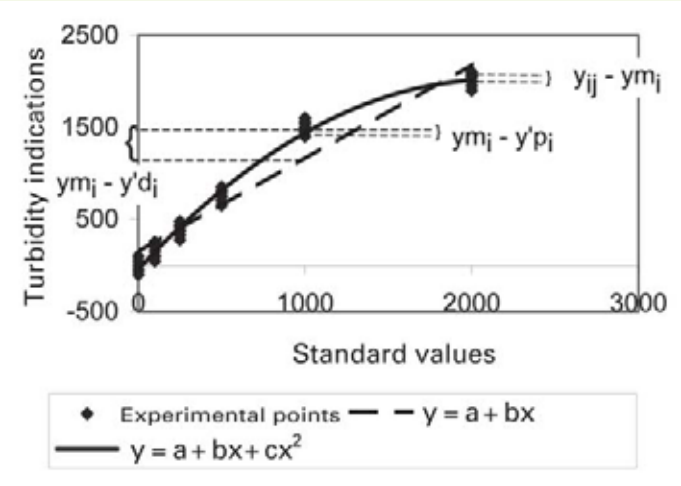

Results and discussion

Figure 3 shows both the standard experimental deviation $s_{exp}(x_0)$ and calibration uncertainties $s_{etal}(x_0)$ for three calibration configurations. As indicated above in the section Equipment and calibration methods, these results correspond to the average of three series of each one of the three configurations, which consist of the following:

❶ linear calibration on five standard ranges (five repetitions);

❷ linearization, by means of modeling with a second-order polynomial on one standard range (five repetitions);

❸ linearization by means of modeling with a second-order polynomial on five standard ranges in order to take their uncertainty into account **[6]**.

This figure demonstrates that:

• The standard uncertainty deviation for polynomial calibrations on either one ❷ or five ❸ standard ranges is significantly less than that of the linear calibration ❶, for which a relative uncertainty of approximately 25% is obtained for the value of 100 FAU and 4% at 500 FAU. The first uncertainty value, which corresponds to the bottom of the turbidity range for urban wastewater, seems too high for some applications: it would thus be preferable to linearize by modeling using a polynomial.
• The standard uncertainty deviation for polynomial calibration on five ranges ❸, which incorporates the uncertainty on standards, appears to be dominant with respect to the standard experimental uncertainty deviation $s_{exp}(x_0)$. The uncertainty on standards therefore plays a key role in calibration uncertainty.

• The standard experimental uncertainty deviation $s_{exp}(x_0)$, which characterizes measurement dispersion, increases as a function of the measured value.
• The standard uncertainty deviation for polynomial calibration on a single range ❷ is notably less than that for the calibration on five ranges ❸, whereas the opposite would be expected: the multiplication of experiments serves to decrease uncertainty on the average values observed and it would be anticipated that the uncertainty on a single range equals $\sqrt{5}$ times higher than on five ranges. The explanation behind this paradox is that calibration on a single range, performed by diluting a parent suspension, does not enable accounting for the uncertainties on the parent suspensions, i.e. for the dispersion in their values.

Figure 3
Standard deviations of experimental and calibration uncertainty for three configurations, compared with measurement repeatability on formazine

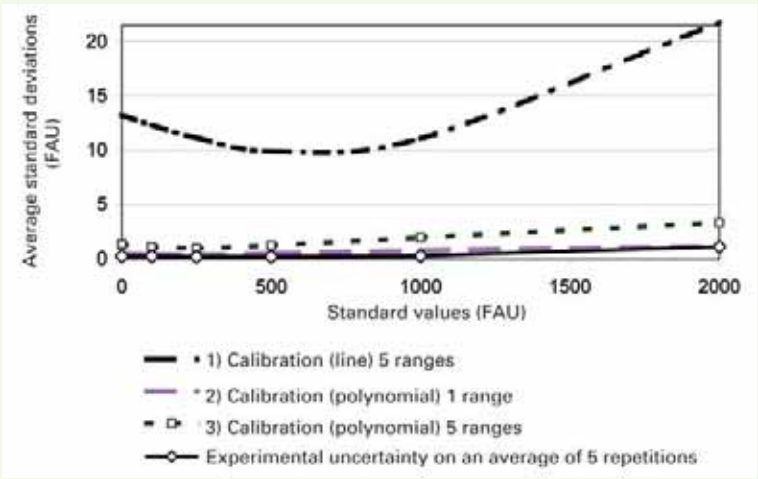

Calculation based on five ranges ❸ proves to be the most satisfactory since it takes into account both calibration curve non-linearity and standard uncertainty. Yet, the calculation still assumes this uncertainty (along with the experimental uncertainty) to be independent of the concerned standard value. Experimental results obtained by turbidity recordings on the standard suspensions prepared by successive dilutions of different parent suspensions (see section entitled *Simulation of standard values*) reveal that this hypothesis has not been satisfied: dispersion increases with the value at a ratio of 1:6 between the levels of 100 and 2,000 FAU.

Variable uncertainties may be handled analytically, but the calculations remain rather complex (see the section *Uncertainty calculation with classical analytical formulas* for the linear calibration) and it was thus decided to proceed with the Monte Carlo calibration simulation method, which is straightforward to implement and remains generic: it allows processing different scenarios similarly, provided sufficient knowledge of the statistical characteristics of each error source.

EVALUATION OF CALIBRATION UNCERTAINTY USING THE MONTE CARLO METHOD

Method principle and implementation

The Monte Carlo method entails describing the statistical distribution of the output variable for a process through running many process simulations, based on random drawings of input variable values depending on their own distributions **[7-9]**.

In our case, the process consists of generating the calibration curve, which is accomplished by the following steps:

❶ Simulation of standard value x_{5k} of the parent suspension (index k) by random drawing according to the experimentally-observed distribution.

❷ Simulation of standard values x_{ik}, obtained for lower levels by successive dilutions of the parent suspension basedon experimentally-observed distribution.

❸ Simulation of average device indications y_{ikm} for the theoretical standard values x_{ik}, by application of the calibration function f deemed to be true (average calibration curve established for the set of fifteen experimental calibration ranges).

❹ Simulation of the individual experimental values measured y_{ijk}, stemming from device repeatability, according to the experimentally-observed repeatability distribution.

❺ Adjustment on the experimental points (x_{ik}, y_{ijk}) of the simulated calibration curve f_k.

❻ Deviation calculation $f_k(x_0) - f(x_0)$ for the current value x_0.

The simulation of a large number of calibration functions f_k yields the deviation distribution between these curves and the true curve.

Calibration curve uncertainty at a given level of confidence (e.g. 95%) is then obtained by calculating the quantile corresponding with the simulated deviation values. Since the deviation distribution turns out to be normal, the 68% quantile corresponds to the standard deviation $s_{etal}(y_0)$.

A detail of the various steps is provided below.

› Simulation of standard value x_{5k} of the parent suspension

The dispersion in parent suspension concentrations was initially evaluated; this step required independently preparing fifteen parent suspensions at 2,000 FAU, in accordance with Standard ISO 7027 **[5]**, and fifteen ranges were prepared by means of successive dilutions, thus making it possible to establish a precise calibration curve. Thanks to their standardized mode of preparation, the standard values of the parent suspensions could be assumed centered on the value 2,000 FAU. The standard deviation $s(x_5$ of dispersion in the standard values (i.e. 10 FAU, *see* **Fig. 4** was then determined by dividing the standard deviation of measurement dispersion over the fifteen parent suspensions by the slope f' of the average calibration function (with these measurements displaying a normal distribution: Shapiro-Wilk test).

The standard value x_{5k} of a parent suspension (index k) can be simulated by random drawing, according to the normal distribution of standard deviation $s(x_5)$ and average 2,000 FAU.

› Simulation of standard values x_{ik} less than the parent suspension value

The variance in the concentration of a standard suspension with a nominal value of x_i, obtained using a parent suspension of value x_5 by means of successive dilutions and leading to an overall dilution by a factor d_i ($x_i = d_i \cdot x_5$), is expressed as follows:

$$s^2(x_i) \simeq d_i^2\, s^2(x_5) + x_5^2\, s^2(d_i) \qquad (3)$$

The first term indicates the effect of uncertainty on the parent suspension, while the second yields the uncertainty on the dilution factor.

In order to evaluate this second term experimentally, turbidity readings were conducted on fifteen standard ranges, prepared from fifteen different parent suspensions. These readings enabled establishing an average calibration curve, which through inverse application then served to evaluate the dispersion in standard values based on the dispersion in turbidity readings. Let x_{ik} be the k^{th} value of the i^{th} level of calibration obtained.

Moreover, x'_{ik} was calculated as the value that would have been obtained from the k^{th} parent suspension in the absence of uncertainty on the dilution:

$$x'_{ik} = d_i^* \cdot x_{5k} = d_i^* \cdot f^{-1}(y_{5k})$$

with y_{5k} read for the k^{th} parent suspension and d_i^* the theoretical dilution factor. It then becomes possible to calculate:

$$\delta_{ik} = x_{ik} - x'_{ik}$$

The deviations δ_{ik} follow a normal distribution and exhibit no bias (Student test). The child suspensions are thus like the parent suspension, i.e. centered on their respective nominal standard values.

It can now be demonstrated that:

$$s^2(\delta_i) \simeq x_5^2\, s^2(\delta_i) = x_i^2\, [s(\delta_i)/\delta_i]^2 \qquad (4)$$

Figure 4 shows the estimations of $s(\delta_i)$ obtained for fifteen ranges, along with the uncertainty affecting these estimations calculated on the basis of a Khi2 law.

Figure 4
Experimental standard deviations on the standard values with respect to the origin (parent suspension or child suspension), compared with measurement repeatability on formazine

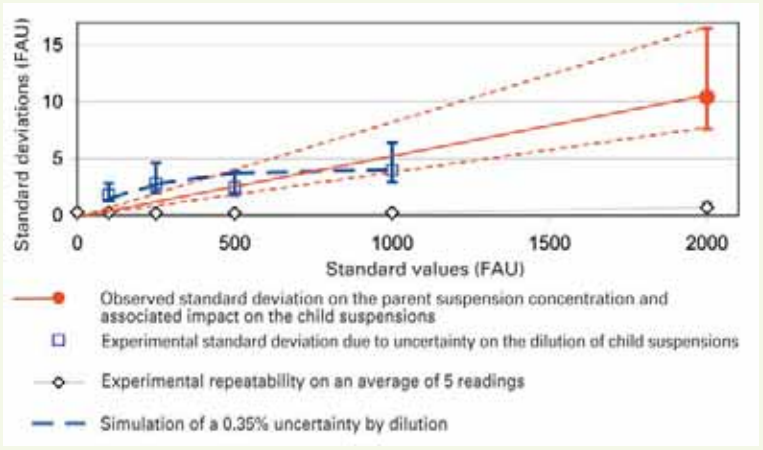

It is seen that $s(\delta_i)$ varies by just a small amount. The values observed are compatible with an uncertainty on the dilutions of 0.35% at each dilution.

In any event, the contribution of uncertainty on the parent suspension concentration remains quite close to that of the dilution uncertainty, with both being considerably greater than the experimental uncertainty.

Here, it becomes possible to simulate the values of the child suspensions x_{ik} by means of successive multiplications of x_{5k} by the dilution factors, with the dilution errors of standard deviation $s(\delta_i)$ added in.

› Simulation of the average device indications y_{ikm}

The average device indications y_{ikm} are simulated by conversion of x_{ik}, using the calibration function f which is deemed to be true. Since the user is not assumed to know the true values x_i, these values are assigned to the theoretical values x_{ik}.

› Simulation of the individual *measured* experimental values y_{ijk}

The individual *measured* y_{ijk} (five repetitions) are simulated based on averages y_{ikm} by applying the device repeatability, characterized by the standard deviation $s_{exp}(y_0) = s_{exp}(x_0) \cdot f'(x_0$, as determined from calibration experiments (see the *Results and discussion* section in Part I of this article and **Fig. 4**). It is to be noted that the standard deviation of repeatability is substantially less than the standard deviations characterizing dispersion and dilution errors, which justifies an evaluation of these two errors under good accuracy conditions.

› Adjustment of the simulated calibration curve f_k

In our case, where uncertainties of repeatability and on standards vary with the measured value, an adjustment of the calibration function (here a polynomial) is carried out so as to minimize the sum **[7]**:

$$\sum_i \sum_j g_i \left(y_{ijk} - f_k(x_i)\right)^2 = \sum_i \sum_j \left(y_{ijk} - f_k(x_i)\right)^2 \cdot \frac{1}{s_i^2(x_i)} \qquad (5)$$

with the weight: $g_i = \frac{1}{s^2_{exp}(x_i) + (f'_k(x_i))^2 s^2(x_i)} = \frac{1}{s^2_t(x_i)}$

Since device repeatability and reproducibility of standards constitute two independent phenomena, the variance $s^2_t(x_i)$ for indication y_i of standard value $_i$, as expressed by the denominator of the weight expression g_i, equals the repeatability variance $s^2_{exp}(x_i)$ plus the variance of x_i converted into an indication variance (multiplied by the slope of the calibration relation $f'_k(x_i)$). This weighting therefore consists of homogenizing the influence of variable dispersion at the experimental points by dividing deviations $(y_{ijk} - f_k(x_i))$ by the standard deviation $s_t(x_i)$ of this dispersion.

Adjusting the simulated calibration curve on the *experimental* points (x_{ik}, y_{ijk}) may be simply performed using a spreadsheet (e.g. the DROITEREG function in Microsoft Excel), but the adjustment functions do not typically allow for weighting. In order to circumvent this difficulty, instead of weighting a number of deviations equal to n_i according to level, it is possible to modulate the number of deviations proportionally with the inverse of the variance $1/ s^2_t(x_i)$. The expression in **(5)** can then be multiplied by a large enough factor F such that the ratios $F/ s^2_t(x_i)$ assume values close to integers N_i. This expression may now be written as:

$$\sum_i \sum_j \left(y_{ijk} - f_k(x_i)\right)^2 \cdot \frac{F}{s^2_t(x_i)} = \sum_i \sum_j \left(y_{ijk} - f_k(x_i)\right)^2 \cdot N_i \qquad (6)$$

It is apparent that in order to weight the deviations analogously with g_i,it is necessary to simulate N_i indications for level i, which can be easily executed in a spreadsheet by copying cells.

› Evaluation of calibration uncertainty

The next step serves to determine deviations between the simulated calibration curves f_k and the reputedly true curve f for the current standard value x_0. The 68% envelope of deviations between curves f_k and curve f provides the confidence zone corresponding to standard deviation $s_{etal}(y_0)$.

Results and discussion

By being based on the standard deviation values of repeatability and dilution error determined from experimental results in the *Results and discussion* section in Part I of this article, a random drawing has been used to simulate a large number (250, which enables evaluating standard deviations to within 10%) of experimental calibration series.

Figure 5 presents the standard calibration deviations $s_{etal}(x_0)$ (equals $s_{etal}(y_0)$ divided by $f'(x_0)$, as explained in the *Uncertainty calculation* section in Part I, to be expressed in standard values), calculated by both classical analytical formulas and the Monte Carlo simulation.

The following can be stated:

– calibration uncertainty on a single range simulated by Monte Carlo is actually on the order of $\sqrt{5}$ times greater than that on five ranges (as anticipated in the Results and discussion section in Part I);

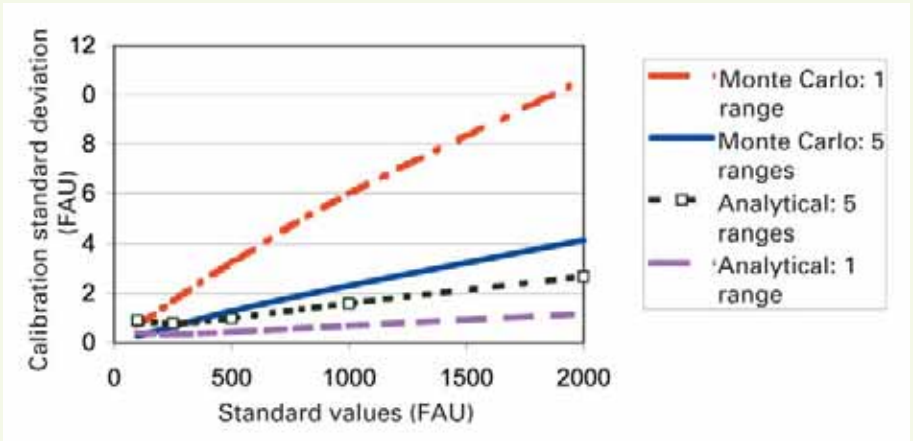

Figure 5
Calibration standard deviations on a single range and on five ranges, as determined by both approximated analytical formulas and the Monte Carlo simulation

– on five ranges, the approximated analytical method overestimates uncertainty for the small values (0.9 FAU vs. 0.3 at 100 FAU) and underestimates it by roughly one third for the average to high values: this finding would be due to the fact that the analytical method does not take into account the variability in variance as a function of the measured value.

Another advantage with the Monte Carlo method is to run additional simulations to confirm the set of hypotheses. As such:

– if a zero uncertainty has been simulated on the parent suspensions, then the standard deviations determined by the analytical method on a single range and on five ranges are similar, which confirms that underestimation on a single range is due to the fact that uncertainty on parent suspensions has not been considered;

– if a constantly residual variance has been simulated, then the standard deviations determined on five ranges using both the analytical and Monte Carlo methods are similar, which confirms that the deviations observed between these two methods are due to the lack of inclusion by the analytical method of variability in the residual variance as a function of the measured value.

TOTAL UNCERTAINTY OF TURBIDITY MEASUREMENT

The variance characterizing total uncertainty is derived by combining calibration variance with experimental variance.

Calibration variance s^2_{etal} was determined in the above section, as was experimental variance s^2_{exp}, within the scope of the formazine calibration. For a given device however, the experimental variance depends on the measurement medium. It has been observed that under identical measurement conditions, the standard deviations s_{ERUi} of repeatability for an urban wastewater sample (ERU) during dry weather vary from 0.8 to 8 FAU over the interval 100-2,000 FAU, which is much greater than for formazine.

In order to determine total measurement uncertainty, calibration variance must therefore be combined with the measured experimental variance, either on formazine (for calibrations, verifications and adjustments) or on wastewater (for establishing relations between pollutants and turbidity). In taking the average of n_0 independent measurements of y_i on the wastewater, the experimental variance s^2_{expERU} corresponding with average turbidity y_{0m} is then expressed as a function of the standard deviation s_{ERU} determined using the same device on this wastewater flow, i.e.:

$$s^2_{exp\,ERU}(x_0) = \frac{s^2_{exp\,ERU}(y_{0m})}{f'(x_0)^2} = \frac{s^2_{ERU}(x_0)}{n_0 \cdot f'(x_0)^2} \qquad (7)$$

Dividing by $f'(x_0)$ was explained in the *Uncertainty calculation* section in Part I by converting the indication y_{0m} into standard value x_0 *via* the inverse of the calibration function **(Fig. 6)**.

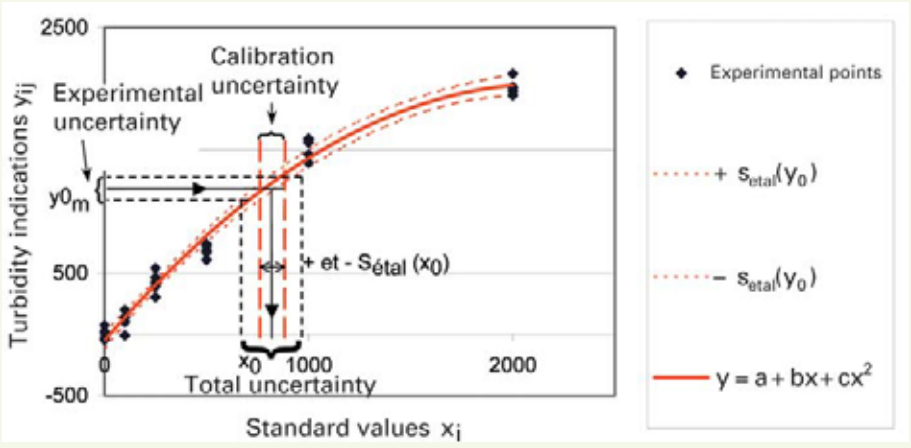

Figure 6
Composition of the experimental standard deviation on y_{0m} and the calibration standard deviation for determining total uncertainty on turbidity measurement x_0

In the general case, the sources of experimental error and calibration error remain independent. Total variance $s^2_{totale}(x_0)$ on the estimation of x_0 is obtained by summing the variances corresponding with these two error sources:

$$s^2_{totale}(x_0) = s^2_{etal}(x_0) + s^2_{expERU}(x_0) \quad (8)$$

The turbidity measurement values on wastewater samples (sieved at 2 mm in order to eliminate the coarse, unrepresentative suspended material) exhibit a normal distribution. The calculated standard deviation of uncertainty is thus assimilated with a 68% confidence interval. To make the transition to the more conventional confidence level of 95%, which corresponds to an α risk of 5% that the value lies outside the confidence interval, this standard deviation is multiplied by a broadening factor corresponding with the $t_{1-\alpha/2}(\nu_{tot})$ Student variable, with ν_{tot} representing the number of degrees of freedom (equal to the number N of calibration readings less the polynomial degree). The result from turbidity measurement x_0 with its total uncertainty is thereby expressed as follows:

$$x_0 \pm s_{totale}(x_0) \cdot t_{1-\alpha/2}(\nu_{tot}) \quad (9)$$

However, since the number n_0 of readings to determine average turbidity differs from the number of calibration measurements N, the number of degrees of freedom required to determine $t_{1-\alpha/2}(\nu_{tot})$ can be calculated by the Welch formula **[7]**:

$$\nu_{tot} = \frac{s^4_{totale}}{\frac{s^4_{etal}}{\nu_{etal}} + \frac{s^4_{expERU}}{\nu_0}} \quad (10)$$

with ν_{etal} equals N less the order of the calibration polynomial and $\nu_0 = n_0$.

It can be concluded from **Figure 7** that the experimental standard deviation on an average of five repetitions $s_{expERU}(x_0)$ lies in the neighborhood of the calibration standard deviation on five ranges $s_{etal}(x_0)$, with the sum of the two leading to a total uncertainty standard deviation of 1 to 8 FAU, i.e. 0.6% to 1% of the measured value.

Figure 8 reveals the degradation in the level of accuracy when proceeding with a calibration on a single range, in assuming that an uncertainty evaluation on the standards has already been produced. This degradation is small since the uncertainties remain less than 1.5%. The maximum gain of a factor of $\sqrt{5}$ has not been reached in this example, especially for lower values, as a result of the sizable experimental uncertainty on urban wastewater.

Figure 7
Standard deviations of total uncertainty, calibration and repeatability for a five-range calibration with an average on five repetitions

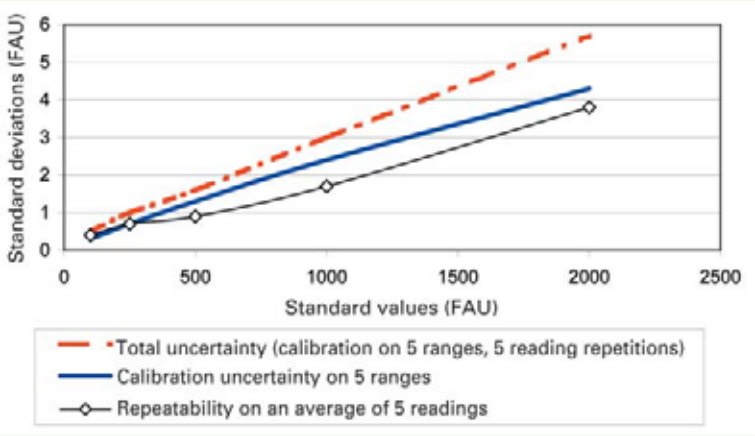

Figure 8
Total relative uncertainties at the 95% confidence level for two types of calibration

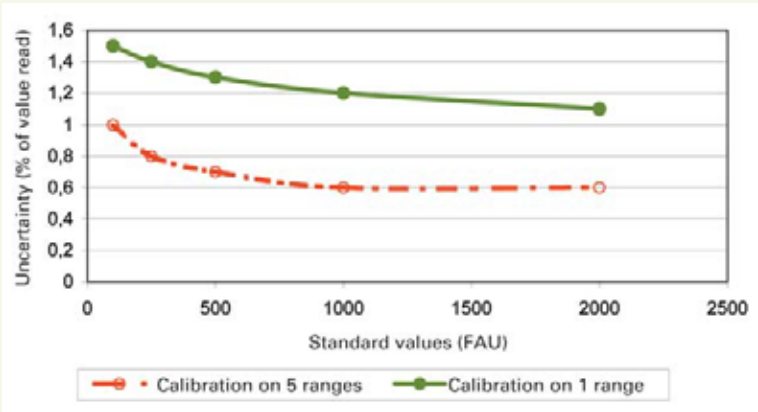

CONCLUSION

The evaluation of turbidity measurement uncertainty using common analytical formulas yields erroneous and often overly optimistic results since:

– the dispersion in measurement values increases with the actual value to be measured;
– these formulas do not account for uncertainty on the standards.

A more evolved analytical method would enable incorporating these elements, but the Monte Carlo method proves simpler to implement. For both methods, it is obviously necessary that all required information has been acquired, e.g. by means of measurements on standard range repetitions, based on different parent suspensions. The Monte Carlo method also facilitates testing the impact of various hypotheses concerning error structures, either for compensating a lack of information or for analyzing potential inadequacies of the classical analytical method. Moreover, the Monte Carlo method is well adapted for linearizations using polynomials higher than the second order.

Lastly, total short-term uncertainty of turbidity measurements on a sample has yielded a very satisfactory outcome (less than 1.5% above 100 FAU), provided that the device has been suitably linearized. Such a result may be obtained under implementation conditions close to those found in the laboratory: control over environmental variables (temperature, luminosity), preparation and conservation of standards, sample homogenization during the measurements. The follow-up study will focus on evaluating long-term uncertainty *in situ*, by taking into account the influence of environmental variables and the drift in the measurement device.

REFERENCES

1 **Maréchal A.**, **Aumond M.**, **Ruban G.**, Mise en œuvre de la turbidimétrie pour évaluer la pollution des eaux résiduaires, *La Houille Blanche*, **5**, **2001**, pp. 81-86.

2 **Bertrand-Krajewski J.-L.**, TSS concentration in sewers estimated from turbidity measurements by means of linear regression accounting for uncertainties in both variables, *Water Science and Technology*, vol. **50**, **11**, **2004**, pp. 81-88.

3 **Ruban G.**, **Bertrand-Krajewski J.-L.**, **Chebbo G.**, **Gromaire M.-C.**, **Joannis C.**, Précision et reproductibilité du mesurage de la turbidité des eaux résiduaires urbaines, *La Houille Blanche*, **4**, **2006**, pp. 129-135.

4 **Aumond M.**, **Joannis C.**, Mesure en continu de la turbidité sur un réseau séparatif d'eaux usées : mise en œuvre et premiers résultats, *La Houille Blanche*, **4**, **2006**, pp. 121-128.

5 ISO 7027, *Water quality – Determination of turbidity*, International Organization for Standardization (ISO), December **1999**, 14 pages.

6 XP T 90-210, Qualité de l'eau – Protocole d'évaluation d'une méthode alternative d'analyse physico-chimique quantitative par rapport à une méthode de référence, AFNOR, Paris (France), décembre **1999**, 61 pages.

7 **Bertrand-Krajewski J.-L.**, **Laplace D.**, **Joannis C.**, **Chebbo G.**, *Mesures en hydrologie urbaine et assainissement*, Technique et Documentation, Paris (France), **2000**, 794 pages.

8 **Neuilly M.**, **CETAMA**, *Modélisation et estimation des erreurs de mesure*, Technique et Documentation, Paris (France), **1998**, 704 pages.

9 **Wonnacot T.H.**, **Wonnacot R.J.**, *Introductory Statistics for Business and Economics (4th edition)*. Ed. John Wiley and Sons, New York (USA), **1990**, 990 pages, ISBN 978-0-471-61517-0.